Singly and doubly excited states of butadiene, acrolein, and glyoxal: Geometries and electronic spectra

Biswajit Saha and Masahiro Ehara[a)]
Department of Synthetic Chemistry and Biological Chemistry, Graduate School of Engineering, Kyoto University, Katsura, Nishikyo-ku, Kyoto 615-8510, Japan

Hiroshi Nakatsuji[a)]
Department of Synthetic Chemistry and Biological Chemistry, Graduate School of Engineering, Kyoto University, Katsura, Nishikyo-ku, Kyoto 615-8510, Japan and Fukui Institute for Fundamental Chemistry, Kyoto University, 34-4 Takano Nishihirakicho, Sakyo-ku, Kyoto 606-8103, Japan

(Received 18 November 2005; accepted 4 April 2006; published online 7 July 2006)

Excited-state geometries and electronic spectra of butadiene, acrolein, and glyoxal have been investigated by the symmetry adapted cluster configuration interaction (SAC-CI) method in their s-*trans* conformation. Valence and Rydberg states below the ionization threshold have been precisely calculated with sufficiently flexible basis sets. Vertical and adiabatic excitation energies were well reproduced and the detailed assignments were given taking account of the second moments. The deviations of the vertical excitation energies from the experiment were less than 0.3 eV for all cases. The SAC-CI geometry optimization has been applied to some valence and Rydberg excited states of these molecules in the planar structure. The optimized ground- and excited-state geometries agree well with the available experimental values; deviations lie within 0.03 Å and 0.7° for the bond lengths and angles, respectively. The force acting on the nuclei caused by the excitations has been discussed in detail by calculating the SAC-CI electron density difference between the ground and excited states; the geometry relaxation was well interpreted with the electrostatic force theory. In Rydberg excitations, geometry changes were also noticed. Doubly excited states (so-called $2\,^1A_g$ states) were investigated by the SAC-CI general-*R* method considering up to quadruple excitations. The characteristic geometrical changes and large energetic relaxations were predicted for these states. © *2006 American Institute of Physics*.
[DOI: 10.1063/1.2200344]

I. INTRODUCTION

The investigations of the spectroscopy and photochemistry of conjugated molecules are unabated in order to clarify the role of conjugation and the electronic properties of their excited states have been of considerable interest for many years. For understanding the spectroscopic properties of π-conjugated molecules, electronic spectra of butadiene, acrolein, and glyoxal are fundamental and an important subject. Therefore, various experimental techniques were applied to characterize the electronic excited states of these molecules. The UV absorption spectra of glyoxal and acrolein were first reported by Walsh and co-workers.[1–3] Later on, electron impact excitation,[4] electron energy loss spectroscopy (EELS),[5–7] UV absorption spectra,[8–10] resonance Raman scattering spectroscopy[11] methods were applied to these molecules. However, in some cases, contradictory results were obtained; for example, in *trans*-butadiene, resonance Raman scattering study showed that $1\,^1B_u$ state is energetically higher than $2\,^1A_g$ state, whereas multiphoton ionization (MPI) or EELS experiments reported the reverse order. Many theoretical works have also been performed to investigate the electronic spectra of these molecules.[12–29] *Ab initio* methods such as the symmetry adapted cluster configuration interaction (SAC-CI),[16] complete active space perturbation theory to second order (CASPT2),[21,22] multireference Moller-Plesset (MRMP),[23] and multireference configuration interaction[24,25] (MRCI) were utilized to calculate the vertical excitation energies of these molecules. In the recent years, the low-lying excited states of *trans*-1,3-butadiene were intensively examined, in particular, the $2\,^1A_g$ and $1\,^1B_u$ excited states by MRCI with singles and doubles (MR-CISD) and multireference averaged quadratic coupled cluster (MR-AQCC) methods[30] and the $2\,^1A_g$ excited state by using a variety of *ab initio* methods, complete active space self-consistent field (CASSCF), CASPT2, multireference singles and doubles configuration interaction (MRSDCI), and quasidegenerate variational perturbation theory (QDVPT).[31]

The geometry relaxation in the excited states is of special interest, since the excited-state geometries are responsible for the shape of the absorption spectra as well as the emission spectra. Accurate theoretical investigation on the excited-state geometries has become possible.[24,27,29] For the present 4π-electron systems, some theoretical works were reported for the stable geometries of the low-lying valence excited states. However, the analytical energy gradients are not so common to the highly correlated methods which describe both static and dynamics correlations. Among corre-

[a)]Authors to whom correspondence should be addressed. Electronic mails: ehara@sbchem.kyoto-u.ac.jp and hiroshi@sbchem.kyoto-u.ac.jp

lated methods, SAC-CI,[32,33] restricted active space self-consistent field (RASSCF),[29] and MRCI[34] energy gradients are available. Therefore, further methodological developments and extensive applications for the excited-state geometries are expected.

For 1,3-butadiene, many theoretical works have been performed for the electronic spectra. Kitao and Nakatsuji[16] studied the valence and low-lying Rydberg states in both *trans* and *cis* forms by using the SAC-CI method. They investigated the vertical excitations and gave the reliable assignments for the optically allowed ^1B_u states. They showed that both σ- and π-electron correlations are important for calculating the various excitations. Calculation by means of linear and quadratic response theories also has been performed for the low-lying levels of this molecule.[35] Recently, second order multireference perturbation theory using an optimized partitioning (MROPT2) was applied to calculate the excited states of butadiene and other molecules.[28] The excited-state geometries of the valence exited states of this molecule were also investigated. Szalay *et al.* studied the planar and nonplanar structures with multiconfiguration self-consistent field (MCSCF).[24] Boggio-Pasqua *et al.* performed the RASSCF calculation to examine the geometries of the ionic and covalent excited states of butadiene.[29]

For acrolein, valence and Rydberg excited states of *cis*- and *trans*-acrolein were recently investigated by using CASPT2 and time-dependent density functional theory (TD-DFT) methods.[27] Accurate assignments were proposed comparing with the experimental results. They also studied the solvent effect of this molecule in aqueous solution. Although the excitation energies estimated by the CASPT2 and TD-DFT methods agree well, the oscillator strength values differ among these calculations. For some transitions, differences were also found in the excitation energies between the CASPT2 and multistate CASPT2 (MS-CASPT2) calculations. They also studied the geometry relaxation of three lowest valence excited states with unconstrained geometry optimizations.

For glyoxal, the SAC-CI method with direct-type algorithm was applied to the singlet and triplet excited states.[19] The adiabatic excitations were also examined and the agreements with the experimental values were encouraging. The excitation energies for this molecule estimated by the SCF,[26] CI,[20] and CASSCF (Ref. 36) calculations are also available for some low-lying excited states; however, the agreement with the experimental values was not good. For this molecule, the electron correlations were found to be important for reproducing the order of the n^+, n^-, $\pi_{C=O^-}$ and $\pi_{C=O^+}$ valence ionized states,[26,37,38] and therefore sufficient electron correlations should be evaluated for the accurate calculations of the excited states.

The SAC-CI method[39,40] has firmed its applicability in the wide varieties of subjects in chemistry and physics, such as in molecular spectroscopy, biological photochemistry, and surface chemistry.[41] The analytical energy gradients of the SAC-CI method are available for various kinds of electronic states.[32,33,42] The method is useful for studying the excited-state geometries, dipole moments, and vibrational frequencies of molecules. In this work, we applied the SAC-CI method to the accurate assignments of the electronic spectra of s-trans 1,3-butadiene, s-*trans* acrolein, and s-*trans* glyoxal up to high energy region and to the investigation of the excited-state geometries of these molecules. The σ- and π-electron correlations which are crucial for the proper description of the ionic and covalent excited states can be well described by the SAC-CI method. By calculating the electron density difference between the ground and excited states with the SAC-CI method, the geometry relaxations in the excited states were discussed based on the electrostatic force (ESF) theory proposed by Nakatsuji.[43]

II. COMPUTATIONAL DETAILS

The excitation energy and the excited-state geometries for the singlet and triplet excited states were calculated. For calculating the vertical excitations, the double-zeta basis sets due to Huzinaga/Dunning[44] plus one polarization $[4s2p1d/2s]$ were adopted with double-zeta Rydberg functions for describing $3s3p3d$ $(2s2p2d)$ and $4s4p$ orbitals $[2s2p]$ (Ref. 45) for butadiene and glyoxal, and $3s3p3d$ $(2s2p2d)$ orbitals for acrolein. Hence, the numbers of atomic orbitals (AOs) were 188, 152, and 180 for butadiene, acrolein, and glyoxal, respectively. The $1s$ orbitals of first-row atoms and their counterpart molecular orbitals are kept fixed and excluded from the active space, and therefore the active spaces for calculating the vertical spectra are 172, 136, and 164 molecular orbitals (MOs).

For the excited-state geometry calculations, we included the $3s3p$ Rydberg functions $[2s2p]$ (Ref. 45) along with DZ1P basis for all these three molecules. The minimum-orbital deformation (MOD) method with frozen-core orbitals was adopted in the SAC-CI geometry optimization. Therefore, the active spaces used in the geometry optimization step are 11 occupied MOs for each molecule and 89, 85, and 81 unoccupied MOs for 1,3-butadiene, acrolein, and glyoxal, respectively.

Since the present valence and Rydberg excited states are dominantly described by single excitations, we used the SD-R calculations. To reduce the computational effort, the perturbation selection scheme was adopted.[46] The LevelThree accuracy was adopted to calculate the large number of excited states accurately. The threshold of the linked terms for the ground state was set to $\lambda_g = 1.0 \times 10^{-6}$. The unlinked terms were described as the product of the linked operators with SDCI coefficients larger than 0.005. For excited states, the threshold of the linked doubles was set to $\lambda_e = 1.0 \times 10^{-7}$. The thresholds of the CI coefficients for calculating the unlinked operators were 0.05 and 0.00 for the R and S operators, respectively.

The SAC-CI geometry optimization was performed with the CI-singles (CIS) optimized parameters as the initial geometry. The initial geometries of CIS calculations were due to experimental ones.[47] The geometry optimizations were restricted to planar structures for all molecules. The SAC-CI general-R calculations,[33,48] including up to quadruple excitations, were also performed for estimating vertical excitation energies and optimized geometries of the doubly excited

TABLE I. Vertical excitation energy (ΔE in eV), oscillator strength (f), and the electronic part of second moment ($\langle r^2 \rangle$ in a.u.) of s-*trans* 1,3-butadiene for various singlet transitions using $[4s2p1d/2s]+[2s2p2d](n=3)+[2s2p](n=4)$ basis set.

State/nature	Expt.	SAC-CI ΔE	SAC-CI f	SAC-CI $\langle r^2 \rangle$	CASPT2[a]	SAC-CI[b] (previous)	MROPT[c]	RASSCF[d]	MR-AQCC[e]	MRSDCI[f]	MR-CC CI-PS[g]	DC-MR SD-CI[h]
$X\ ^1A_g$			0.0000	341.9								
$2\ ^1A_g$ $(V, \pi_{C=C^*})$[i]		6.56	0.0000	351.9	6.27[a,j]	7.05	6.83	6.93	6.60 6.55	6.24 6.78	6.53	6.40
$3\ ^1A_g$ $(\pi_{C=C} \rightarrow 3d_{yz})$	7.48[k]	7.47	0.0000	490.0	7.47	7.38						
$4\ ^1A_g$ $(\pi_{C=C} \rightarrow 3d_{xz})$	7.80[k]	7.84	0.0000	549.2		7.86						
$5\ ^1A_g$ $(\pi_{C=C} \rightarrow 4d_{yz})$		8.22	0.0000	661.1								
$6\ ^1A_g$ $(\pi_{C=C} \rightarrow 4d_{xz})$		8.57	0.0000	576.6								
$1\ ^1B_g$ $(\pi_{C=C} \rightarrow 3s)$	6.21[l]	6.18	0.0000	395.0	6.29				6.32			
$2\ ^1B_g$ $(\pi_{C=C} \rightarrow 3d_{x^2-y^2})$	7.28,[k] 7.30[l]	7.28	0.0000	471.4	7.30							
$3\ ^1B_g$ $(\pi_{C=C} \rightarrow 3d_{xy})$		7.33	0.0000	467.8								
$4\ ^1B_g$ $(\pi_{C=C} \rightarrow 3d_{z^2})$		7.42	0.0000	465.9								
$5\ ^1B_g$ $(\pi_{C=C} \rightarrow 4s)$		7.64	0.0000	579.6								
$6\ ^1B_g$ $(\pi_{C=C} \rightarrow 4d_{x^2-y^2})$		8.05	0.0000	730.8								
$7\ ^1B_g$ $(\pi_{C=C} \rightarrow 4d_{xy})$		8.13	0.0000	674.8								
$8\ ^1B_g$ $(\pi_{C=C} \rightarrow 4d_{z^2})$		8.19	0.0000	613.1								
$1\ ^1A_u$ $(\pi_{C=C} \rightarrow 3p_x)$	6.64[l]	6.45	0.0000	396.2	6.56				6.56			
$2\ ^1A_u$ $(\pi_{C=C} \rightarrow 3p_y)$	6.80[l]	6.65	0.0350	424.4	6.69				6.74			
$3\ ^1A_u$ $(\pi_{C=C} \rightarrow 4p_x)$		7.70	0.0017	572.4								
$4\ ^1A_u$ $(\pi_{C=C} \rightarrow 4p_y)$		7.78	0.0098	637.8								
$5\ ^1A_u$ $(\pi_{C=C} \rightarrow 4f_{x^2y})$		7.93	0.0000	595.6								
$6\ ^1A_u$ $(\pi_{C=C} \rightarrow 4f_{xy^2})$		7.97	0.0001	585.2								
$7\ ^1A_u$ $(\pi_{C=C} \rightarrow 4f_{yz^2})$		8.05	0.0066	546.0								
$8\ ^1A_u$ $(\pi_{C=C} \rightarrow 4f_{xz^2})$		8.14	0.0000	533.4								
$1\ ^1B_u$ $(V, \pi_{C=C})$	5.92,[k] 6.25[m]	6.33	0.6467	366.1	6.23	6.43	6.52	6.60	6.36			
$2\ ^1B_u$ $(\pi_{C=C} \rightarrow 3p_z)$	7.07[k]	7.08	0.2453	413.8	6.70	7.08			7.02			
$3\ ^1B_u$ $(\pi_{C=C} \rightarrow 4p_y)$	7.86[l]	7.90	0.0016	587.9	7.79	7.91						
$4\ ^1B_u$ $(\pi_{C=C} \rightarrow 4f_{x^2z})$	8.00[k]	8.05	0.0059	526.8								
$5\ ^1B_u$ $(\pi_{C=C} \rightarrow 4f_{xyz})$	8.18[l]	8.12	0.0176	549.9								
$6\ ^1B_u$ $(\pi_{C=C} \rightarrow 4f_{z^3})$		8.14	0.0061	532.1								

[a]Reference 21.
[b]Reference 16.
[c]Reference 28.
[d]Reference 29.
[e]Reference 30.
[f]References 24 and 25.
[g]Reference 55.
[h]Reference 31.
[i]SAC-CI general-R calculation.
[j]Reference 51.
[k]References 4–6.
[l]References 9 and 53.
[m]Reference 10.

states. The GAUSSIAN 03 suite of programs[49] has been utilized for the SAC-CI calculations. Interested readers may glean much information from the articles[41] and references therein.

III. ELECTRONIC SPECTRA OF S-*TRANS* 1,3-BUTADIENE

In this section, we first discuss the valence and Rydberg excited states of s-*trans* 1,3-butadiene. The SAC-CI results of the singlet and triplet excited states are summarized for the vertical excitations in Tables I and II, respectively, with the experimental and other theoretical values. The calculated ionization threshold is 8.80 eV with the present basis set in comparison with the experimental one, 9.09 eV.[50] The deviations of the vertical excitation energies from the experimental values are less than 0.3 eV in all cases. For the single photon process, the transitions to A_u or B_u states are optically allowed and the transitions to g-symmetry state are forbidden.

Strong absorption for the $1\ ^1B_u$ state was observed experimentally at 6.25 eV,[10] which is 0.08 eV lower than our value of 6.33 eV. Other theoretical values for this transition are 6.60 eV (Ref. 29) (RASSCF), 6.23 eV,[21,22] 6.06 eV (Ref. 51) (CASPT2), 5.90 eV (Ref. 52) (TDDFT), and 6.18 eV (Ref. 30) (MR-AQCC). Thus most of the recent theoretical values are converging at 6.2 eV for this ionic state. From the SD-R calculations, we found that the contributions of doubly excited configurations were significant to the $2\ ^1A_g$ state. Hence, for this state, we performed the SAC-CI general-R calculations and obtained a value of 6.56 eV. This state, as reported by Doering and McDiarmid,[9,53] is of valence character, which corroborates our result. Some experiments have assigned this state at quite low energy, ranging from a value of 5.4 to 5.8 eV.[11,54] The EELS experiment reported a value of 7.08 eV (Ref. 4) or 7.3 eV (Refs. 5 and 9) for this state. Our value is in good agreement with the value (6.53 eV) obtained by the MR consistent correlation CI perturbation

TABLE II. Vertical excitation energy (ΔE in eV) and the electronic part of second moment ($\langle r^2 \rangle$ in a.u.) of s-*trans* 1,3-butadiene for triplet transitions by the SAC-CI method with $[4s2p1d/2s]+[2s2p2d](n=3)+[2s2p](n=4)$ basis set.

State/nature	Expt.[a,b]	SAC-CI ΔE	SAC-CI $\langle r^2 \rangle$	MRCI[c]	SAC-CI[d] (previous)
$1\,^3A_g$ $(V, \pi_{C=C^+})$	4.91	5.08	344.1	4.95	5.15
$2\,^3A_g$ $(\pi_{C=C^-} \rightarrow 3s)$		7.36	444.2		7.22
$3\,^3A_g$ $(\pi_{C=C^-} \rightarrow 3d_{yz})$		7.42	474.7		7.26
$4\,^3A_g$ $(\pi_{C=C^-} \rightarrow 3d_{xz})$		7.99	477.2		
$5\,^3A_g$ $(\pi_{C=C^-} \rightarrow 4d_{yz})$		8.17	590.1		
$6\,^3A_g$ $(\pi_{C=C^-} \rightarrow 4d_{xz})$		8.57	655.1		
$1\,^3B_g$ $(\pi_{C=C^-} \rightarrow 3s)$		6.14	393.4	6.17	
$2\,^3B_g$ $(\pi_{C=C^-} \rightarrow 3d_{x^2-y^2})$		7.26	470.2	7.29	
$3\,^3B_g$ $(\pi_{C=C^-} \rightarrow 3d_{xy})$		7.32	464.0		
$4\,^3B_g$ $(\pi_{C=C^-} \rightarrow 3d_{z^2})$		7.40	464.2		
$5\,^3B_g$ $(\pi_{C=C^-} \rightarrow 4s)$		7.62	576.2		
$6\,^3B_g$ $(\pi_{C=C^-} \rightarrow 4d_{x^2-y^2})$		8.04	728.8		
$7\,^3B_g$ $(\pi_{C=C^-} \rightarrow 4d_{xy})$		8.12	670.2		
$8\,^3B_g$ $(\pi_{C=C^-} \rightarrow 4d_{z^2})$		8.16	617.9		
$1\,^3A_u$ $(\pi_{C=C^-} \rightarrow 3p_x)$		6.45	396.5	6.48	
$2\,^3A_u$ $(\pi_{C=C^-} \rightarrow 3p_y)$	6.81	6.61	421.3	6.67	
$3\,^3A_u$ $(\pi_{C=C^-} \rightarrow 4p_x)$		7.69	565.3		
$4\,^3A_u$ $(\pi_{C=C^-} \rightarrow 4p_y)$		7.76	558.0		
$5\,^3A_u$ $(\pi_{C=C^-} \rightarrow 4f_{x^2y})$		7.77	429.2		
$6\,^3A_u$ $(\pi_{C=C^-} \rightarrow 4f_{xy^2})$		7.92	592.9		
$7\,^3A_u$ $(\pi_{C=C^-} \rightarrow 4f_{yz^2})$		7.97	586.6		
$8\,^3A_u$ $(\pi_{C=C^-} \rightarrow 4f_{xz^2})$		8.04	542.6		
$1\,^3B_u$ $(V, \pi_{C=C^-})$	3.22	3.20	342.5	3.24	3.48
$2\,^3B_u$ $(\pi_{C=C^-} \rightarrow 3p_z)$		6.79	418.0	7.55	6.65
$3\,^3B_u$ $(\pi_{C=C^-} \rightarrow 4p_z)$		7.89	584.8	7.92	7.83
$4\,^3B_u$ $(\pi_{C=C^-} \rightarrow 4f_{x^2z})$		8.03	561.7		
$5\,^3B_u$ $(\pi_{C=C^-} \rightarrow 4f_{xyz})$		8.06	524.8		
$6\,^3B_u$ $(\pi_{C=C^-} \rightarrow 4f_{z^3})$		8.13	522.4		

[a]References 4–6.
[b]Reference 2.
[c]Reference 17.
[d]Reference 16.

selected (MR-CCCI-PS),[55] and 6.40 eV of DC-MRSDCI (Ref. 31) and 6.55 eV of MR-AQCC calculations.[30] MROPT (Ref. 28) calculation estimated this state at 6.83 eV, MRS-DCI estimated value of 6.77 eV,[25] and CASPT2 calculation reported a value of 6.27 eV.[21] The CASPT2 tends to predict low excitation energy, especially for the doubly excited states.

Analyzing the electronic part of the second moment $\langle r^2 \rangle$, we found that both the $1\,^1B_u$ state with $\langle r^2 \rangle = 366.1$ a.u. and the $2\,^1A_g$ state with $\langle r^2 \rangle = 351.9$ a.u. have purely valence character as reported in the previous studies. By including σ- and π-electron correlations, reliable values of $\langle r^2 \rangle$ can be obtained for these ionic and covalent states. The z component of the second moment was calculated to be $\langle z^2 \rangle = 35.5$ a.u. for the $1\,^1B_u$ state and $\langle z^2 \rangle = 73.0$ a.u. for the $2\,^1B_u$ state. In the previous SAC-CI calculation,[16] these values were $\langle z^2 \rangle = 44$ and 65 a.u., for the $1\,^1B_u$ and $2\,^1B_u$ states, respectively. Kitao and Nakatsuji[16] showed that π- and σ-electron correlations are important for the ionic valence excited states of *trans*-butadiene and the wave function of the ionic valence excited state expands like a Rydberg state without σ-electron correlations. In the present calculation, therefore, the σ-electron correlation was also well described.

We obtained the ionic $1\,^1B_u$ state energetically lower than the covalent $2\,^1A_g$ state which is supported by most of the previous computations and experiments. The oscillator strength was calculated to be 0.65 for the $1\,^1B_u$ state in comparison with the observed[56] value ($\approx$0.4) and the previous SAC-CI (Ref. 16) value (0.47) showed quite good agreement. The present oscillator strength is in good agreement with the CASCI value of 0.69 of Serrano-Andres *et al.*[21] It differs, however, by an order from the corresponding value of 0.07 by Buenker *et al.*[57] with MRCI. The oscillator strength of 0.245 for the $2\,^1B_u$ state agrees well with the previous SAC-CI (Ref. 16) value of 0.234.

Next, we discuss the Rydberg excited states, which are calculated in high accuracy by the SAC-CI method. As compared in Tables I and II, the present results agree very well with the experimental values. We calculated the $2\,^1B_u$ state at 7.08 eV as $\pi_{C=C^-} \rightarrow 3p_z$ Rydberg transition which agrees very well with the experimental value, 7.07 eV.[4–6] Other $3p$ Rydberg transitions were obtained at 6.45 and 6.65 eV in A_u symmetry, for x and y components, respectively, whose oscillator strengths are small. Rydberg $3s$ state, $1\,^1B_g$, was calculated to be 6.18 eV, in good agreement with the experimental value of 6.21 eV.[9,53] Transitions to $3d$ Rydberg states are all dipole forbidden, A_g and B_g states, and they were calculated in the energy region of 7.28–7.84 eV above the ground state. The $3d_{x^2-y^2}$, $3d_{yz}$, and $3d_{xz}$ states were calculated to be 7.28, 7.47, and 7.84 eV, in comparison with the experimental[4–6] values of 7.28, 7.48, and 7.80 eV, respectively.

For the transitions to $n=4$, Rydberg $4s$, $4p$, and $4d$ states were obtained in the energy regions of 7.64, 7.70–7.90, and 8.05–8.57 eV, respectively. Since the Rydberg functions of lower angular momentum was placed on each carbon, Rydberg $4f$ states were described in the present calculation. We also confirmed the present assignment by other SAC-CI calculations with $4f$ Rydberg function placed on the center of molecule. Experimentally, Doering and McDiarmid[9] reported an optically allowed Rydberg ($4f$) transition at 8.18 eV. We have assigned this transition to $\pi_{C=C} \rightarrow 4f_{xyz}$ state calculated at 8.12 eV.

Now, we discuss the triplet excited states corresponding to the singlet excited states for which we performed calculations. The lowest two triplet states, i.e., $1\,^3B_u$ and $1\,^3A_g$, were observed experimentally[4,5] and the theoretical results show good agreement with the experiment; the present values are 3.20 and 5.08 eV, in comparison with the experimental values of 3.22 and 4.91 eV, respectively. For the triplet Rydberg states, Price and Walsh[2] reported the transition at 6.81 eV, which was assigned to the $\pi_{C=C^-} \rightarrow 3s$ Rydberg transition. For this transition, we calculated the $3p_y$ triplet excited state ($2\,^3A_u$ state) at 6.61 eV. The CI calculation performed by Shih *et al.*[17] reported a value of 6.67 eV for the same transition, which agrees well with the present values. Our assignment of $\pi_{C=C^-} \rightarrow 3p_z$ for the $2\,^3B_u$ state also corroborates the previous SAC-CI assignment $3p\pi$ by Kitao and Nakatsuji;[16] the excitation energy differs by an amount of 0.14 eV.

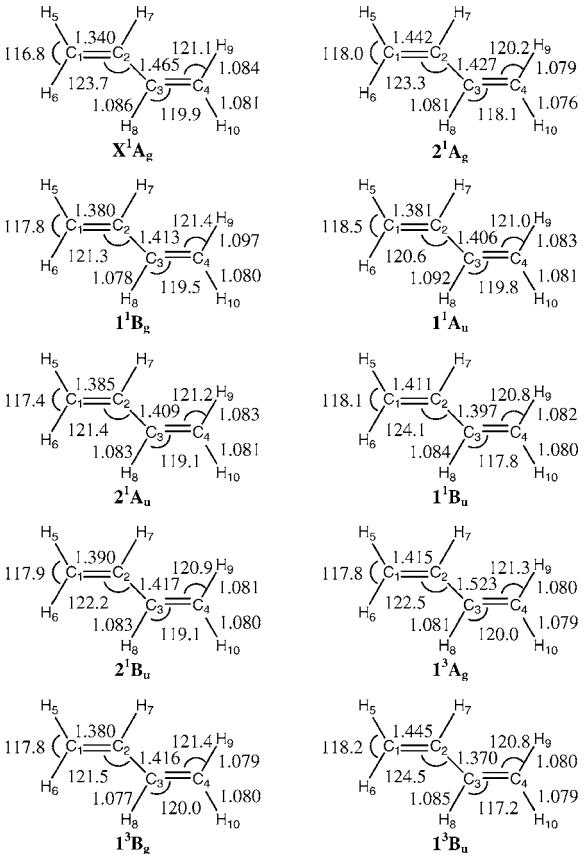

FIG. 1. Geometries for the ground and excited states of s-*trans* 1,3-butadiene optimized by the SAC-CI method. Bond lengths and angles are in Å and degree, respectively.

IV. GROUND- AND EXCITED-STATE GEOMETRIES OF S-*TRANS* 1,3-BUTADIENE

The equilibrium geometries for the ground and some excited states of butadiene optimized by the SAC-CI method are displayed in Fig. 1. The ground state of *trans*-butadiene has the planar C_{2h} structure and the excited-state geometries are examined with restricting the C_{2h} structure, though nonplanar structures were reported to be stable in some excited states.[29] Recently, it was reported that the T_1 ($1\,^3B_u$) state of butadiene has planar structure.[58] In Table III, we summarized the comparison of the C–C bond length and CCC bond angles with the experimental and other theoretical values. The adiabatic transition energies are given in Table IV.

The optimized ground-state geometry is in excellent agreement with the experimental one.[47] The terminal $C_1{=}C_2$ bond length is deviated by only 0.005 Å from the experimental value and we got the same $C_2{-}C_3$ bond length as the experimental one. The RASSCF calculation[29] showed deviations of 0.011 and 0.003 Å for $C_1{=}C_2$ and $C_2{-}C_3$ bond lengths, respectively, while the CASPT2 (Ref. 59) estimation deviates by 0.008 and 0.011 Å. The CCC bond angle in the present study shows the deviation of 0.5° from the experimental value.

For the excited states, planar C_{2h} structure is interesting to examine the large geometrical change, although stable nonplanar structures were found in some excited states, for example, the C_2 structure was found to be a minimum in the

TABLE III. Comparison of optimized geometries for s-*trans* 1,3-butadiene using $[4s2p1d/2s]+[2s2p](n=3)$ basis set. Bond length and angle are in Å and degree, respectively.

State/nature	Method	C=C	C–C	∠CCC
$X\,^1A_g$	SAC-CI	1.340	1.465	123.8
	Expt.[a]	1.345	1.465	123.3
	RASSCF[b]	1.351	1.468	123.9
	CASPT2[c]	1.348	1.454	123.6
$2\,^1A_g$ ($V, \pi_{C=C^+}$)	SAC-CI[d]	1.442	1.427	123.3
	RASSCF[b]	1.501	1.421	123.0
	CASPT2[c]	1.499	1.418	123.4
$1\,^1B_u$ ($V, \pi_{C=C^-}$)	SAC-CI	1.411	1.397	124.1
	RASSCF[b]	1.414	1.495	122.2
	CASPT2[c]	1.421	1.399	124.1
$1\,^3B_u$ ($V, \pi_{C=C^-}$)	SAC-CI	1.445	1.370	124.5
	MCQR[e]	1.457	1.361	124.3
$1\,^3A_g$ ($V, \pi_{C=C^+}$)	SAC-CI	1.415	1.523	122.5
	MCQR[e]	1.435	1.477	122.9

[a]Reference 47.
[b]Reference 29.
[c]Reference 59.
[d]SAC-CI general-*R* calculation.
[e]Reference 77.

RASSCF work by Boggio-Pasqua *et al.*[29] For the doubly excited valence $2\,^1A_g$ state, we performed the SAC-CI general-*R* optimization. For this state C=C bond length increases by 0.102 Å and the C–C bond length decreases by 0.035 Å. The C=C bond length is deviated by ~0.059 Å from that of the CASPT2 (1.501 Å) and RASSCF (1.499 Å) estimations.[29] But the C–C bond length and ∠CCC show good agreement.

Noticeable elongations by 0.071, 0.105, and 0.075 Å of the $C_1{=}C_2$ bond length were calculated for the other va-

TABLE IV. Adiabatic and vertical excitation energy (in eV) for excited states of s-*trans* 1,3-butadiene using $[4s2p1d/2s]+[2s2p](n=3)$ basis set.

State/nature	Method	Vertical	Adiabatic
$2\,^1A_g$ ($V, \pi_{C=C^+}$)	SAC-CI[a]	6.56	5.38
	CASSCF[b]	6.63	5.30
	CASPT2[b]	6.25	5.02
	RASSCF[c]	6.93	5.81
	CASPT2[d]	···	5.37
$1\,^1B_u$ ($V, \pi_{C=C^-}$)	SAC-CI	6.36	6.03
	Expt.[e]	···	5.73
	Expt.[f]	6.25	···
	CASPT2[d]	···	6.18
	RASSCF[c]	6.60	6.22
	MRCI[g]	6.70	6.44
$2\,^1B_u$ ($\pi_{C=C^-} \rightarrow 3p_z$)	SAC-CI	7.13	6.91
$3\,^1B_u$ ($\pi_{C=C^-} \rightarrow 4p_z$)	SAC-CI	8.21	7.96
$1\,^1A_u$ ($\pi_{C=C^-} \rightarrow 3p_x$)	SAC-CI	6.50	6.29
$2\,^1A_u$ ($\pi_{C=C^-} \rightarrow 3p_y$)	SAC-CI	6.68	6.46
$1\,^1B_g$ ($\pi_{C=C^-} \rightarrow 3s$)	SAC-CI	6.17	5.99
$1\,^3B_u$ ($V, \pi_{C=C^-}$)	SAC-CI	3.21	2.62
$1\,^3A_g$ ($V, \pi_{C=C^+}$)	SAC-CI	5.07	4.70
$1\,^3B_g$ ($\pi_{C=C^-} \rightarrow 3s$)	SAC-CI	6.12	5.94

[a]SAC-CI general-*R* calculation.
[b]Reference 31.
[c]Reference 29.
[d]Reference 59.
[e]Reference 60; Nonplanar conformation.
[f]Reference 10.
[g]References 24 and 25.

lence excited states, $1\ ^1B_u$, $1\ ^3B_u$, and $1\ ^3A_g$, respectively. For the $1\ ^3B_u$ and $1\ ^3B_u$ states, the C_2-C_3 bond lengths were calculated to shrink by 0.068 and 0.095 Å, respectively, while the C_2-C_3 bond length of $1\ ^3A_g$ state elongated by 0.058 Å. The SAC-CI geometries of the $1\ ^1B_u$ state in C_{2h} structure are in fairly good agreement with those of CASPT2 by Page and Olivucci[59] and RASSCF (Ref. 59) calculations. Discrepancy was found for only the ∠CCC in the RASSCF calculation by an amount of 1.9°. The $C_1{=}C_2$ bond length increases for every excited state due to the reduction in bond order and this is more clearly explained by the SAC-CI density difference as discussed below. The change in ∠CCC is not unique among the excited states. For $1\ ^1B_u$ and $1\ ^3B_u$ states, the CCC bond angle increases slightly and for other cases it decreases as shown in Fig. 1.

Among the triplet excited states for which SAC-CI geometry optimization was performed, the maximum energy lowering due to geometry relaxation is obtained for the $1\ ^3B_u$ state as 0.59 eV. The energy lowering for the $1\ ^1B_u$ and $1\ ^3A_g$ states were calculated to be 0.33 and 0.37 eV, respectively. Adiabatic energy for the $1\ ^1B_u$ state in C_{2h} structure has been examined by several authors. The CASPT2 calculation predicted it as 6.18 eV,[59] and the RASSCF calculation placed it at 6.22 eV.[29] These values deviate by ~0.2 eV from the present value of 6.03 eV, whereas the MRCI gave much higher energy, 6.44 eV.[24] Experimentally, the adiabatic excitation energy for the $1\ ^1B_u$ state was measured as 5.73 eV,[60] which is lower than the theoretical values; nonplanar C_2 structure should be responsible for this energy. The $2\ ^1A_g$ state showed large relaxation energy, 1.18 eV, because of large geometry change such as the increase of the $C_1{=}C_2$ ($C_3{=}C_4$) bond length by 0.102 Å. Adiabatic transition energy for this state obtained in the present calculation is 5.38 eV which is in agreement with the CASSCF value of 5.30 eV.[31] The CASPT2 calculated values are 5.02 eV (Ref. 31) and 5.37 eV.[59]

The SAC-CI geometry optimization was also performed for several Rydberg excited states in C_{2h} structure; the geometry changes of the Rydberg states were smaller than those of the valence excited states as expected. For the Rydberg states, the elongation of the $C_1{=}C_2$ bond is around 0.04–0.05 Å, while for the valence excited states it is around 0.1 Å as mentioned above. Similarly, the change in the C_2-C_3 bond length is larger for the valence states than the Rydberg states. The electron density distribution is much more affected by the valence excitation than the Rydberg excitation. The C–H bonds decrease in length in the excited states. The HC_1H bond angles increase by 0.6°–1.7°, while C_4C_3H bond angles decrease by 0.1°–2.7° in the excited states.

These changes in the geometry due to excitation can be explained using ESF theory proposed by Nakatsuji.[43] We discuss here some of the geometry changes in the excited states of butadiene based on the ESF theory. The electron density differences between the ground and excited states are shown in Fig. 2. The electron density in the $C_1{=}C_2$ ($C_3{=}C_4$) bond region decreases and that in the C_2-C_3 bond region increases. More precisely, the electron density in the σ-bond region increases and the density in the π-bond region decreases in general. As a consequence, the $C_1{=}C_2$ ($C_3{=}C_4$) bond increases in length and the C_2-C_3 bond decreases. For the excited $1\ ^1B_u$ and $1\ ^3B_u$ states comparatively large increment in electron density was obtained which is supported by the change in C_2-C_3 bond. Similarly, the C_2-H_7 bond decreases in length for the $1\ ^1B_g$ and $1\ ^3B_g$ excited states due to an increase of electron density along this bond region. Because of the decrement of electron density in the $C_1{=}C_2$ ($C_3{=}C_4$) bond region, the exchange (EC) force along this bond decreases, resulting to an increment of the $\angle HC_1H$ ($\angle HC_4H$) for all the excited states.

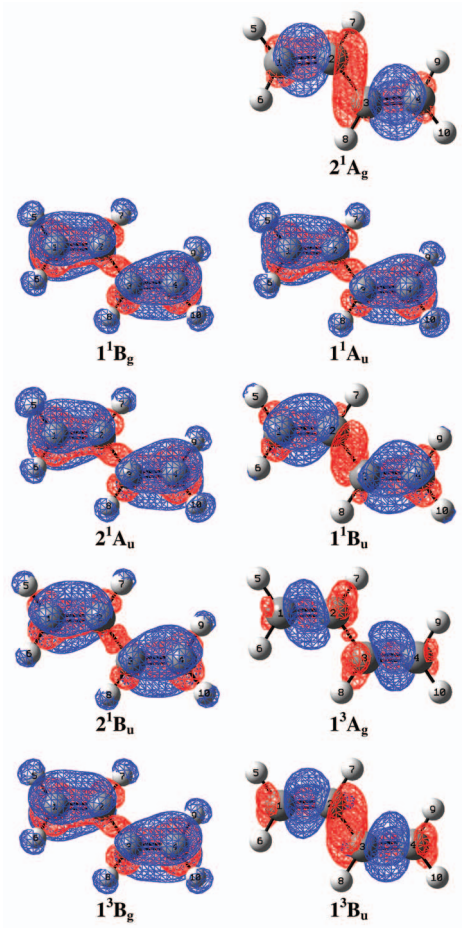

FIG. 2. (Color) SAC-CI electron density difference between the ground and excited states of s-*trans* 1,3-butadiene. Blue: decrement; red: increment (interval=0.003).

V. ELECTRONIC SPECTRA OF S-*TRANS* ACROLEIN

The SAC-CI results of the singlet and triplet excited states of acrolein for vertical transition are summarized in Tables V and VI, respectively. The first ionization potential (IP) obtained from the present calculation was 9.82 eV, in comparison with the experimental value of 10.10 eV.[50] The Hartree-Fock orbital sequence of acrolein is expressed as $(12a')^2(1a'')^2(13a')^2(2a'')^2(3a'')^0$ and the absorption of acrolein is due to the π electrons and nonbonding oxygen electrons, i.e., excitations from the $2a''$ and $13a'$ MOs, respectively. Therefore, valence excited states of $2a''\rightarrow 3a''(A'',\pi\rightarrow\pi^*)$, $13a'\rightarrow 3a''(A'',n\rightarrow\pi^*)$, and Rydberg excited states appear below the ionization threshold.

TABLE V. Vertical excitation energy (ΔE in eV), oscillator strength (f), and the electronic part of second moment ($\langle r^2 \rangle$ in a.u.) for the singlet transitions in s-*trans* acrolein using $[4s2p1d/2s]+[2s2p2d](n=3)$ basis set.

State/nature	Expt.[a] ΔE	SAC-CI ΔE	SAC-CI F	SAC-CI $\langle r^2 \rangle$	CASPT2[b] ΔE	CASPT2[b] f	MS-CASPT2[b] ΔE	TDDFT[b]
$X\ ^1A'$				299.5				
$2\ ^1A'$ $(V, \pi_{C=C})$	6.42	6.92	0.3660	314.3	6.94	0.6550	6.10	
$3\ ^1A'$ $(V, \pi_{C=O})$		8.16	0.0948	310.5	7.43	0.0140	7.80	8.20
$4\ ^1A'$ $(n_O \rightarrow 3s)$	7.10	7.19	0.2355	336.6	6.75	0.0390	6.97	
$5\ ^1A'$ $(n_O \rightarrow 3p_y)$	7.58	7.61	0.0420	357.5	7.39	0.0110	7.55	
$6\ ^1A'$ $(n_O \rightarrow 3p_x)$	7.77	7.83	0.0072	381.6	7.26	0.0680	7.49	
$7\ ^1A'$ $(\pi_{C=C} \rightarrow 3p_z)$	8.37	8.48	0.0078	354.0	8.04	0.0470	7.91	
$8\ ^1A'$ $(\pi_{C=C} \rightarrow 3d_{xz})$	8.49	8.58	0.0118	443.0	7.73	0.0050	8.45	
$9\ ^1A'$ $(n_O \rightarrow 3d_{x^2-y^2})$		8.60	0.0004	425.5	8.19	0.0001	9.18	
$10\ ^1A'$ $(n_O \rightarrow 3d_{z^2})$		8.69	0.0024	434.8	8.27	0.0018	9.29	
$11\ ^1A'$ $(n_O \rightarrow 3d_{xy})$		8.80	0.0013	462.0	7.92	0.0120	8.29	
$12\ ^1A'$ $(\pi_{C=C} \rightarrow 3d_{yz})$		8.84	0.0545	374.2	9.32	0.0580	9.44	
$1\ ^1A''$ (V, n_O)	3.77	3.83	0.0001	298.7	3.63	0.0000	3.63	
$2\ ^1A''$ (V, n_O)		7.40	0.0000	315.7	6.26	0.0006	6.26	
$3\ ^1A''$ $(\pi_{C=C} \rightarrow 3s)$	7.77	7.67	0.0546	348.6	7.76	0.0520	7.76	
$4\ ^1A''$ $(n_O \rightarrow 3p_z)$		7.86	0.0013	356.8	7.74	0.0006	7.74	
$5\ ^1A''$ $(\pi_{C=C} \rightarrow 3p_x)$		8.13	0.0003	348.8	8.27	0.0000	8.26	
$6\ ^1A''$ $(\pi_{CH_2} \rightarrow 3p_z)$		8.55	0.0003	324.3	8.66	0.0006	8.65	
$7\ ^1A''$ $(\pi_{C=C} \rightarrow 3d_{z^2})$	8.39	8.59	0.0022	368.7	9.48	0.0000	9.48	
$8\ ^1A''$ $(n_O \rightarrow 3d_{yz})$		8.62	0.0000	417.9	8.58	0.0001	8.46	
$9\ ^1A''$ $(n_O \rightarrow 3d_{xz})$		8.93	0.0000	416.5	8.45	0.0000	8.58	
$10\ ^1A''$ $(\pi_{C=C} \rightarrow 3d_{x^2-y^2})$		9.14	0.0142	372.3	9.36	0.0007	9.36	
$11\ ^1A''$ $(\pi_{C=C} \rightarrow 3d_{xy})$		9.30	0.0000	416.2	9.58	0.0090	9.58	

[a]Reference 3.
[b]Reference 27.
[c]SAC-CI general-R calculation.

Walsh[3] reported the absorption spectra of the valence and various Rydberg states for s-*trans* acrolein. The present results of the vertical transition energies are in good agreement with the values of Walsh. The only other observed transition energy for the lowest $1\ ^1A''$ state was reported by Becker *et al.*[12] We calculated this lowest singlet state at 3.83 eV which shows a fairly good agreement with the observed values, 3.76 (Ref. 3) and 3.75 eV.[12] This is a valence excitation from n_O orbital with very small oscillator strength of 0.0001. Historically, Dykstra and Schaefer III (Ref. 61) studied the low-lying singlet and triplet states of acrolein by the ΔSCF method and calculated lower excitation energies. Very recently, a detailed theoretical investigation on the electronic spectra of acrolein was performed by Aquilante *et al.*[27] using the CASPT2 and TDDFT levels of theories. Excitation energies for the lowest $1\ ^1A''$ state were estimated as 3.63, 3.63, and 3.66 eV by using CASPT2, MS-CASPT2, and TDDFT, respectively. The oscillator strength for this transition was calculated to be 0.000 23 by TDDFT.

Lowest $\pi \rightarrow \pi^*$ excitation, $2\ ^1A'$ state, was observed at 6.42 eV,[3] which is lower than our computed value of 6.92 eV. The MS-CASPT (Ref. 27) calculation estimated this state at 6.10 eV whereas CASPT2 and TDDFT (Ref. 27) predicted this state at 6.94 and 6.35 eV, respectively. This state corresponds to the $1\ ^1B_u$ state of butadiene, isoelectronic molecule, calculated at 6.33 eV. We obtained this transition dominantly as valence character which is in agreement with the CASPT2 result,[27] although this state interacts with

TABLE VI. Vertical transition energy (ΔE in eV) and the electronic part of second moment ($\langle r^2 \rangle$ in a.u.) for the triplet states in s-*trans* acrolein using $[4s2p1d/2s]+[2s2p2d](n=3)$ basis set.

State/nature	SAC-CI ΔE	SAC-CI $\langle r^2 \rangle$	CASPT2[a] ΔE	CASSCF[a] ΔE
$1\ ^3A'$ $(V, \pi_{C=C})$	3.87	300.4	3.81	3.93
$2\ ^3A'$ $(V, \pi_{C=O})$	6.21	299.9		
$3\ ^3A'$ $(n_O \rightarrow 3s)$	6.70	342.1		
$4\ ^3A'$ $(n_O \rightarrow 3p_y)$	7.21	351.4		
$5\ ^3A'$ $(n_O \rightarrow 3p_x)$	7.44	373.5		
$6\ ^3A'$ $(\pi_{C=C} \rightarrow 3p_z)$	8.12	392.7		
$7\ ^3A'$ $(\pi_{C=C} \rightarrow 3d_{yz})$	8.14	354.4		
$8\ ^3A'$ $(n_O \rightarrow 3d_{x^2-y^2})$	8.43	476.2		
$9\ ^3A'$ $(n_O \rightarrow 3d_{xy})$	8.57	520.0		
$10\ ^3A'$ $(\pi_{C=C} \rightarrow 3d_{xz})$	8.63	342.8		
$11\ ^3A'$ $(n_O \rightarrow 3d_{z^2})$	8.65	536.4		
$1\ ^3A''$ (V, n_O)	3.61	298.8	3.39	3.73
$2\ ^3A''$ $(\pi_{C=C} \rightarrow 3s)$	7.36	335.0		
$3\ ^3A''$ $(n_O \rightarrow 3p_z)$	7.65	347.6		
$4\ ^3A''$ $(\pi_{C=C} \rightarrow 3p_x)$	7.90	347.4		
$5\ ^3A''$ $(\pi_{CH_2} \rightarrow 3p_z)$	8.25	343.3		
$6\ ^3A''$ $(n_O \rightarrow 3d_{xz})$	8.32	395.0		
$7\ ^3A''$ $(\pi_{C=C} \rightarrow 3d_{xy})$	8.34	375.1		
$8\ ^3A''$ $(V, \sigma_{C=O})$	8.53	301.5		
$9\ ^3A''$ $(n_O \rightarrow 3d_{yz})$	8.87	483.0		
$10\ ^3A''$ $(\pi_{C=C} \rightarrow 3d_{z^2})$	8.90	384.0		
$11\ ^3A''$ $(\pi_{C=C} \rightarrow 3d_{x^2})$	9.01	495.7		

[a]Reference 27.

$n_O \rightarrow 3s$ transition as seen from the second moments and the oscillator strengths. This mixing of Rydberg character was also reported experimentally in some previous studies.[15,62] Two more valence excited states, $2\ ^1A''$ and $3\ ^1A'$ at 6.26 and 7.43 eV, respectively, were also reported in the CASPT2 calculation.[27] We also got transitions of valence character at 7.40 eV ($2\ ^1A'', n_O \rightarrow \pi^*$) and 8.16 eV ($3\ ^1A', n_{C=O} \rightarrow \pi^*$). The TDDFT, CASPT2, and MS-CASPT2 methods estimated the $3\ ^1A'$ state at 8.20, 7.43, and 7.80 eV, respectively.[27] For $2\ ^1A''$ state, the discrepancy between the present and CASPT2 values is quite large; even the higher R operators by general-R calculation did not have effect on the result.

Several Rydberg states are also calculated and the theoretical excitation energies are in excellent agreement with the experimental values; this agreement can be recognized by the comparison with the CASPT2 results.[27] The excitations from n_O to Rydberg $3s$, $3p_y$, and $3p_x$ were calculated as 7.19, 7.61, and 7.83 eV, respectively, in comparison with the experimental values of 7.10, 7.58, and 7.77 eV, respectively.[3] The transitions from π orbital were predicted in higher energy region, reflecting the binding energies as 8.48 and 7.67 eV for $\pi \rightarrow 3p_z$ and $\pi \rightarrow 3s$ states, respectively, and the corresponding experimental values are 8.51 and 7.75 eV, respectively.[3] We also calculated the transitions to Rydberg $3d$ states and the oscillator strength of these transitions are reasonably small as seen in Table V. Comparing with the assignments by the CASPT2 calculation, the molecular axis is different between the present and CASPT2 works, otherwise the present assignment almost agree with the CASPT2 assignments.[27] However, for some Rydberg states, the calculated excitation energies are very different from the CASPT2 values. It was noted that the MS-CASPT2 is reliable for these Rydberg states.[27] We also compared the MS-CASPT2 (Ref. 27) values in Table V and found better agreement for these Rydberg excitations. However, still a large difference, ~0.6 eV, exists for some Rydberg states, e.g., $^1A'(n_O \rightarrow 3d_{z^2})$ and $^1A'(n_O \rightarrow 3d_{xy})$. The assignments for a few higher Rydberg states are also different. We believe that the SAC-CI results for Rydberg states are reliable based on many previous calculations.[63]

For the triplet excited states, the lowest triplet $1\ ^3A''(n_O \rightarrow \pi^*)$ state was calculated to be 3.61 eV. The CASSCF and CASPT2 calculations reported values as 3.73 and 3.39 eV, respectively.[27] We estimated the second triplet state, $1\ ^3A'(\pi_{C=C} \rightarrow \pi^*)$, at 3.87 eV, which is in good agreement with the previous theoretical results, CASSCF (3.93 eV) and CASPT2 (3.81 eV).[27] We also calculated higher triplet excited states of Rydberg transitions, which are 0.2–0.5 eV lower than the corresponding singlet excited states. Unfortunately, there are no experimental and theoretical information for the higher triplet states for this molecule.

VI. GROUND– AND EXCITED-STATE GEOMETRIES OF S-*TRANS* ACROLEIN

Optimized geometries for the ground state and several excited states of s-*trans* acrolein are displayed in Fig. 3 and the comparison of geometries has been done in Table VII. The adiabatic transition energies are shown in Table VIII.

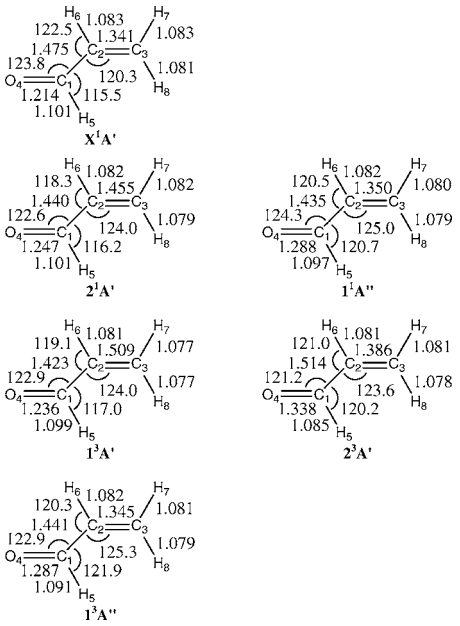

FIG. 3. Geometries for the ground and excited states of s-*trans* acrolein optimized by the SAC-CI method. Bond lengths and angles are in Å and degree, respectively.

The ground state geometry agrees very well with the experimental geometry due to Blom and Bauder.[62] The C_1-C_2, $C_2=C_3$, and $C_1=O$ bond lengths of the ground state agree within 0.005, 0.004, and 0.005 Å, respectively, with the corresponding experimental values, while $\angle C_1C_2C_3$ and $\angle C_2C_1O$ are deviated by 0.5° and 0.4°, respectively. The present results for the ground state show good agreement with the CASPT2.[27]

The excited-state geometries were examined by the CASPT2 (Ref. 27) method for three low-lying singlet and triplet states; $1\ ^1A''$ and $1\ ^3A''$ states were found to be planar and $1\ ^3A'$ state nonplanar. The SAC-CI geometry optimization was performed for five excited states of valence character, namely, $1\ ^1A''$, $2\ ^1A'$, $1\ ^3A'$, $2\ ^3A'$, and $1\ ^3A''$ states in the planar structure. Among these states, the $1\ ^3A'$ and $2\ ^3A'$ states, both of which correspond to $\pi \rightarrow \pi^*$ transition, were calculated to be lowered by 0.41 and 0.64 eV, respectively, due to geometry relaxation. In the case of $1\ ^1A''$ state we adopted the localized molecular orbital (LMO) method to compute the adiabatic transition energy. Using LMO we obtained improvement of the transition energy, 3.38 eV, which is deviated by 0.33 eV from the corresponding experimental result of 3.05 eV.[64] For the other states, $2\ ^1A'$, and $1\ ^3A''$ states, the energy stabilizations due to geometry relaxation were quite small 0.03–0.1 eV. We got a value of 3.42 eV for the $1\ ^3A''$ state, corresponding available experimental value is 3.01 eV.[14] In the ΔSCF calculation,[61] the energy obtained lowering for $1\ ^3A'$ and $1\ ^3A''$ states were as large as 1.11 and 0.68 eV, respectively.

For the first singlet excited $1\ ^1A''$ state, good agreement was obtained between the experimental and computed geometrics. In this case, we got the same values as the experiment for the $C_2=C_3$ bond length and $\angle C_1C_2C_3$.[64] The C_1-C_2 and $C_1=O$ bond lengths are deviated by 0.025 and 0.032 Å, respectively, from the experimental values.[64] For all

TABLE VII. Comparison of optimized geometries of ground and four excited states for s-*trans* acrolein using $[4s2p1d/2s]+[2s2p]$ $(n=3)$ basis set. The bond length and bond angle are in Å and degree, respectively.

State/nature	Method	C_1-C_2	$C_2=C_3$	$C_1=O$	$\angle C_1C_2C_3$	$\angle C_2C_1O$
$X\,^1A'$	SAC-CI	1.475	1.341	1.214	120.3	123.8
	Expt.[a]	1.470	1.345	1.219	119.8	123.4
	CASPT2[b]	1.467	1.344	1.222	120.5	124.2
	PBE0[b]	1.471	1.332	1.204	120.7	124.4
$1\,^1A''$ (V,n_O)	SAC-CI	1.435	1.350	1.288	125.0	124.3
	Expt.[c]	1.460	1.350	1.320	125.0	125.0
	CASPT2[b]	1.381	1.393	1.342	123.0	120.0
$1\,^3A'$ $(V,\pi_{C=C})$	SAC-CI	1.423	1.509	1.236	124.0	122.9
	CASPT2[b]	1.437	1.457	1.231	···	···
$1\,^3A''$ (V,n_O)	SAC-C1	1.441	1.345	1.287	125.3	122.9
	CASPT2[b]	1.393	1.380	1.328	···	···

[a]Reference 62.
[b]Reference 27.
[c]Reference 64.

the excited states reported here, the C_1-C_2 bond was predicted to be contracted relative to the ground state whereas the change in $C_1=O$ bond was negligible. For the $2\,^1A'$ and $1\,^3A'$ states the $C_2=C_3$ bond increases by 0.114 and 0.168 Å, respectively. This is a clear evidence of $\pi_{C=C} \rightarrow \pi^*$ transition. A noticeable change, 3.7°, of the $\angle C_1C_2C_3$ was also predicted for these states, whereas the $\angle C_2C_1O$ is changed by 1.2° and 0.9°, respectively. Similarly, $1\,^1A''$ and $1\,^3A''$ states correspond to $n_O \rightarrow \pi^*$ transition where an elongation of $C_1=O$ bond length by 0.074 Å and an increment of the $\angle C_2C_1C_3$ by 4.7° and 5°, respectively, were obtained. Most of the SCF optimized geometries of Dykstra and Schaefer III (Ref. 61) for excited states agree with the present data. However, there are deviations in some cases. For example, in the excited $1\,^3A'$ state, the $C_1=O$ bond length is deviated by 0.16 Å. The C–H bonds decrease in length in the excited states. Large decrement of the $\angle C_1C_2H$ was obtained, 1.5°–4.2°, in particular for the $2\,^1A'$ excited state, 4.2°. On the other hand, the C_2C_1H bond angles opened around 1°–6°; maximum change, 6°, was obtained for the excited $1\,^3A''$ state.

For acrolein, we also calculated the electron density difference and applied the ESF theory to interpret the geometrical changes. The SAC-CI electronic density differences are displayed in Fig. 4. For the $2\,^1A'$ and $1\,^3A'$ states, the electron density decreases in the π region of $C_2=C_3$ bond. Hence, the change of EC force occurs and the $C_2=C_3$ bond length increases. The opposite effect was obtained for the C_1-C_2 bond due to the increase of electron density in this σ-bond region. The $\angle C_1C_2C_3$ increases also due to the change in the EC force. On the other hand, the $\angle C_2C_1O$ decreases slightly due to the change in atomic dipole (AD) force as the electron density of the lone pair of oxygen increases. The $C_1=O$ bond increases whereas the C_1-C_2 bond decreases as the changes in the electron density and consequently the changes in the EC force in these bond regions are opposite.

TABLE VIII. Adiabatic excitation energy (in eV) of s-*trans* acrolein using $[4s2p1d/2s]+[2s2p]$ $(n=3)$ basis set.

State/nature	Vertical SAC-CI	Adiabatic		
		Expt.	SAC-CI	CASPT2[a]
$1\,^1A''$ (V,n_O)	3.84	3.05[b]	3.38	3.12
$2\,^1A'$ $(V,\pi_{C=C})$	6.95		6.92	
$1\,^3A'$ $(V,\pi_{C=C})$	3.73		3.32	1.46
$2\,^3A'$ $(V,\pi_{C=O})$	6.04		5.40	
$1\,^3A''$ (V,n_O)	3.53	3.01[c]	3.42	2.92

[a]Reference 27.
[b]Reference 64.
[c]Reference 14; 0-0 transition energies.

VII. ELECTRONIC SPECTRA OF S-*TRANS* GLYOXAL

Vertical transition energies below the ionization threshold of s-*trans* glyoxal are summarized in Tables IX and X for singlet and triplet states, respectively. The first IP was calculated to be 10.49 eV, in agreement with the experimental value of 10.60 eV.[50] Glyoxal has delocalized π electrons and

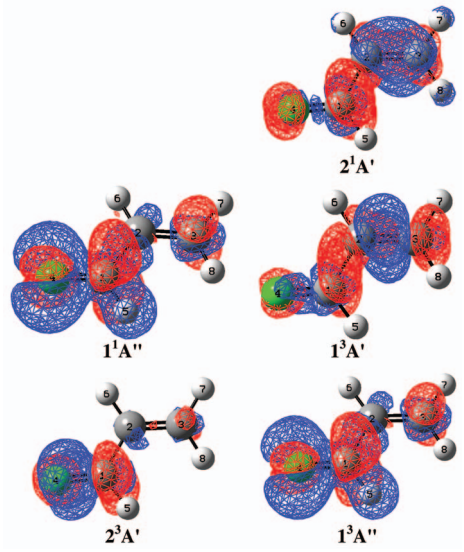

FIG. 4. (Color) SAC-CI electron density difference between the ground and excited states of s-*trans* acrolein. Blue: decrement; red: increment (interval=0.003).

TABLE IX. Vertical excitation energy (ΔE in eV), oscillator strength (f), and the electronic part of second moment ($\langle r^2 \rangle$ in a.u.) for the singlet transitions in s-*trans* glyoxal using $[4s2p1d/2s]+[2s2p2d](n=3)+[2s2p](n=4)$ basis set.

State/nature	Expt. ΔE	SAC-CI ΔE	SAC-CI f	SAC-CI $\langle r^2 \rangle$	SAC-CI[a] (previous)	CASSCF[b]
$X\ ^1A_g$		0.00		268.8		
$2\ ^1A_g\ (V, n_{O^+2})$[c]		5.66	0.0000	269.4		
$3\ ^1A_g\ (n_{O^+} \rightarrow 3s)$[c]		6.55	0.0000	343.9		
$4\ ^1A_g\ (n_{O^+} \rightarrow 3d_{z2})$		8.83	0.0000	358.0		
$5\ ^1A_g\ (n_{O^+} \rightarrow 3d_{x^2-y^2})$		9.03	0.0000	400.2		
$6\ ^1A_g\ (n_{O^+} \rightarrow 4s)$		9.07	0.0000	415.1		
$7\ ^1A_g\ (n_{O^+} \rightarrow 3d_{xy})$		9.24	0.0000	463.0		
$1\ ^1B_g\ (V, n_{O^-})$	4.2,[d] 4.46,[e] 4.63[f]	4.68	0.0000	267.3	4.97	4.36
$2\ ^1B_g\ (V, n_{O^+})$	7.10,[g] 7.45[h]	7.54	0.0000	272.7		
$3\ ^1B_g\ (n_{O^+} \rightarrow 3d_{xz})$		9.03	0.0000	388.7		
$4\ ^1B_g\ (n_{O^+} \rightarrow 3d_{yz})$		9.16	0.0000	416.0		
$5\ ^1B_g\ (\sigma_{CO^+} \rightarrow 3p_z)$		9.77	0.0000	408.5		
$1\ ^1A_u\ (V, n_{O^-})$	2.8[d]	3.10	0.0002	267.2	3.53	3.21
$2\ ^1A_u\ (n_{O^+} \rightarrow 3p_z)$		8.11	0.0026	325.4		
$3\ ^1A_u\ (V, \sigma_{CO^-})$		8.83	0.0004	270.5		
$4\ ^1A_u\ (V, \sigma_{CO^-})$		9.24	0.0013	284.1		
$5\ ^1A_u\ (n_{O^+} \rightarrow 4p_z)$		9.39	0.0020	516.3		
$1\ ^1B_u\ (n_{O^+} \rightarrow 3p_x)$	7.9[d]	7.83	0.0889	316.1	9.78	
$2\ ^1B_u\ (n_{O^+} \rightarrow 3p_y)$		8.17	0.0362	326.8		
$3\ ^1B_u\ (V, \pi_{C=O^-})$		8.86	0.4311	271.7		
$4\ ^1B_u\ (n_{O^+} \rightarrow 4p_x)$		9.28	0.0253	511.6		
$5\ ^1B_u\ (n_{O^+} \rightarrow 4p_y)$		9.34	0.0247	508.2		

[a]Reference 19.
[b]Reference 36.
[c]SAC-CI general-R calculation.
[d]Reference 7.
[e]Reference 78.
[f]Reference 66.
[g]References 1 and 70.
[h]Reference 69.

lone-pair electrons on the oxygen atom. The lone pair orbitals constitute n^+ and n^- orbitals. The valence MOs are n^+, n^-, $\pi_{C=O^-}$, and $\pi_{C=O^+}$ in the order of increasing IP experimentally proposed by Turner,[37] which is in agreement with the present SAC-CI results. The previous systematic SAC-CI study[65] on the valence shell of 4π-conjugated molecules also gave the same ordering for these states. Therefore, the excitations corresponding to $\pi \rightarrow \pi^*$ transition are relatively higher in energy than those of $n \rightarrow \pi^*$; the order of valence shell is important for the correct assignments of the excited states.

The first singlet and triplet A_u $(n \rightarrow \pi^*)$ states were experimentally observed and well established. We have calculated these states at 3.10 and 2.63 eV which deviate by 0.30 and 0.13 eV, respectively, from the corresponding observed values, 2.8 and 2.5 eV;[7] the agreement is better than the previous SAC-CI calculation.[19] The valence $1\ ^1B_g$ state was calculated at 4.68 eV in the present calculation and was characterized as the excitation from the n_{O^+} orbital. This result is corroborated by some experimental works such as the electron-impact spectroscopy of Verhaart and Brongersma;[7] the experimental values were reported as 4.2,[7] 4.46,[66] and 4.63 eV (Ref. 67) for this state. This state was also reported by other theoretical calculations,[18] however, the estimated values range widely as 3.47,[18] 3.96,[68] 4.97,[19] and 4.36 eV.[36]

In higher energy region, we obtained the Rydberg transition $1\ ^1B_u$ $(n^+ \rightarrow 3p_x)$ at 7.83 eV which agrees with the observed state at 7.9 eV by Verhaart and Brongersma,[7] but,

TABLE X. Vertical excitation energy (ΔE in eV) and the electronic part of second moment ($\langle r^2 \rangle$ in a.u.) for the triplet transitions in s-*trans* glyoxal using $[4s2p1d/2s]+[2s2p2d](n=3)+[2s2p](n=4)$ basis set.

State/nature	Expt.[a] ΔE	SAC-CI ΔE	SAC-CI $\langle r^2 \rangle$	SAC-CI[b] (previous)	CI[c]	CASSCF[d]
$1\ ^3A_g\ (V, \pi_{C=O^+})$		6.31	268.1			
$2\ ^3A_g\ (n_{O^+} \rightarrow 3s)$		7.39	308.6			
$3\ ^3A_g\ (n_{O^+} \rightarrow 3d_{z2})$		8.74	339.2			
$4\ ^3A_g\ (n_{O^+} \rightarrow 3d_{x^2-y^2})$		8.98	382.8			
$5\ ^3A_g\ (n_{O^+} \rightarrow 4s)$		9.04	421.7			
$6\ ^3A_g\ (n_{O^+} \rightarrow 3d_{xy})$		9.23	451.1			
$1\ ^3B_g\ (V, n_{O^-})$	3.8	4.12	267.2	4.13	4.58	3.64
$2\ ^3B_g\ (V, n_{O^+})$		7.42	271.8			
$3\ ^3B_g\ (V, \sigma_{CO^+})$		8.85	275.5			
$4\ ^3B_g\ (n_{O^+} \rightarrow 3d_{xz})$		9.03	381.3			
$5\ ^3B_g\ (n_{O^+} \rightarrow 3d_{xz})$		9.20	403.7			
$1\ ^3A_u\ (V, n_{O^+})$	2.5	2.63	267.1	2.9	2.86	2.53
$2\ ^3A_u\ (V, \sigma_{CO^-})$		8.05	267.8			
$3\ ^3A_u\ (n_{O^+} \rightarrow 3p_z)$		8.09	324.4			
$4\ ^3A_u\ (V, n_{O^-})$		8.91	270.1			
$5\ ^3A_u\ (n_{O^+} \rightarrow 4p_z)$		9.37	525.6			
$1\ ^3B_u\ (V, \pi_{C=O^-})$	5.2	5.35	267.6	5.43	5.11	
$2\ ^3B_u\ (n_{O^+} \rightarrow 3p_x)$		7.65	307.5			
$3\ ^3B_u\ (n_{O^+} \rightarrow 3p_y)$		8.06	319.4			
$4\ ^3B_u\ (n_{O^+} \rightarrow 4p_x)$		9.21	488.3			
$5\ ^3B_u\ (n_{O^+} \rightarrow 4p_y)$		9.29	501.4			

[a]Reference 7.
[b]Reference 19.
[c]Reference 20.
[d]Reference 36.

TABLE XI. Comparison of optimized geometries for the ground state of s-*trans* glyoxal using $[4s2p1d/2s]+[2s2p](n=3)$ basis set. Bond length and angle are in Å and degree, respectively.

State/nature	Method	C–C	C=O	∠CCO	∠CCH
$X\,^1A_g$	SAC-CI	1.527	1.208	121.1	114.9
	Expt.[a]	1.530	1.205	120.9	113.7
	Expt.[b]	1.527	1.202	121.2	115.5
	CCSD[c]	1.524	1.203	121.2	115.4
$1\,^1A_u\ (V,n_{O^+})$	SAC-CI	1.500	1.227	123.8	113.6
	Expt.[a]	1.481	1.242	123.6	112.3
	Expt.[b]	1.460	1.252	123.7	114.0
	EOMEE-CCSD[c]	1.496	1.229	123.5	114.0

[a]Reference 74.
[b]Reference 75.
[c]Reference 76.

their assignment was different as $\pi\rightarrow\pi^*$ transition. Robin[69] assigned a diffuse band at 7.75 eV in Walsh's[1,70] optical spectrum to $n^+\rightarrow 3p$ Rydberg state. We also performed the general-*R* calculations for the lowest two states of A_g symmetry. We obtained the valence $2\,^1A_g$ state at a value of 5.66 eV and $3\,^1A_g$ $(n^+\rightarrow 3s)$ Rydberg transition at a value of 6.55 eV. Leclerq *et al.*[18] reported a low value of 4.95 eV for the $2\,^1B_g$ state. Robin[69] assigned the $n^+\rightarrow 3s$ Rydberg state at 7.45 eV. But we assigned this peak as the valence $2\,^1B_g$ state which we obtained at 7.54 eV.

The low-lying triplet states were predicted in the order of $^3A_u<{}^3B_u<{}^3B_g$ in SCF (Ref. 71) and the previous SAC-CI calculations,[19] whereas in the present SAC-CI and previous CI (Ref. 20) studies, the ordering of the levels was calculated to be $^3A_u<{}^3B_g<{}^3B_u$. We obtained a very strong $\pi\rightarrow\pi^*$ valence transition $3\,^1B_u$ with the oscillator strength of 0.431, however, there is no experimental evidence for this transition, since this state lies in high energy region just below the ionization threshold.

VIII. GROUND—AND EXCITED-STATE GEOMETRIES OF S-*TRANS* GLYOXAL

Comparison of the optimized geometries with the available experimental and other theoretical values has been made in Table XI. Optimized geometries and adiabatic excitation energies are displayed in Fig. 5 and Table XII, respectively. Herzberg[72] reported that S_0, S_1, and T_1 states of *trans*-glyoxal have C_{2h} planar structure. This planar structure for the S_0 and S_1 states of s-*trans* glyoxal was also confirmed by other experimental works.[73,74] Again, the SAC-CI ground state geometry agrees very well with the experimental observations of Paldus and Ramasay[74] and Briss *et al.*[75] Deviations of the C–C and C=O bond lengths from experimental values are 0.003 and 0.008 Å, respectively.[75] ∠CCO and ∠CCH also deviate very less from the experimental values, within 0.1° and 0.6°, respectively.[75] The CCSD calculation of Stanton and Gauss[76] for the ground state of glyoxal using TZ2P basis set also gave the same results.

Experimental geometry due to Paldus and Ramasay[74] for the ^1A_u excited state agrees well with our computed geometries. In the excited states, the C=O bond is elongated and the CC bond decreases in length. The increments of the

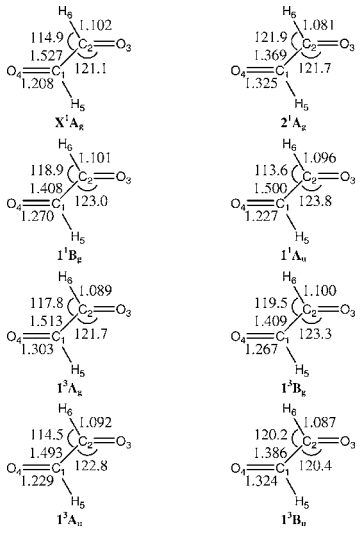

FIG. 5. Geometries for the ground and excited states of s-*trans* glyoxal optimized by the SAC-CI method. Bond lengths and angles are in Å and degree, respectively.

C=O bond length are 0.062, 0.095, and 0.116 Å for the $1\,^1B_g$, $1\,^3A_g$, and $1\,^3B_u$ states, respectively. The corresponding decrements in the C–C bond length are 0.119, 0.014, and 0.141 Å, respectively. The CCH bond angles are increased by 4°, 4.6°, and 5.3°, respectively, for these states, although the change of the CCO bond angles are comparatively small, 2°, 2.2°, and 0.7°, respectively. For the doubly excited $2\,^1A_g$ state, the general-*R* optimization was performed and large relaxation energy was obtained, 1.77 eV. This is due to significant changes in the C=O and C–C bond lengths, by 0.117 and 0.156 Å, respectively. Large amount of energy lowering, 0.75 and 1.22 eV, due to geometry relaxation was also calculated for the $1\,^3A_g$ and $1\,^3B_u$ states, respectively. Similar trend was reported by the previous SAC-CI calculation[19] and CI calculations[20,61] for the $1\,^3B_u$ state. On the other hand, the energy lowering for the $1\,^1B_g$ states was small, although the geometry change was large. Good agreement was obtained for the adiabatic transition energy of the $1\,^3B_g$ state with the previous SAC-CI calculation.[19] However, the present adiabatic transition energy deviates by 0.26 eV from previous SAC-CI calculation for the $1\,^1B_g$ state.

The C=O bond length increases due to a reduction in bond order while the C–C bond distance contracts and the CCO and CCH angles open. The C–H bond lengths shrink in the excited states. To interpret these geometry changes using ESF theory, we have displayed, in Fig. 6, the electron density difference between the ground and excited states. For these excitations, the electron density in the C–C σ-bond region increases. As a result EC force increases along the C–C bond, and the C–C bond length decreases. On the other hand, in the C=O π-bond region, the electron density decreases and the C=O bond length increases. Again the change of the electron density on O atoms results to a change of AD force. Hence, the CCH bond angles increases. A shrink in the C–H bond lengths is also observed due the change of EC force.

TABLE XII. Adiabatic excitation energy (in eV) for the excited states of s-*trans* glyoxal using $[4s2p1d/2s]+[2s2p](n=3)$ basis set.

	SAC-CI		SAC-CI[a] (previous)		SCF[b]		CI[c]	
State/nature	Vertical	Adiabatic	Vertical	Adiabatic	Vertical	Adiabatic	Vertical	Adiabatic
$2\,^1A_g\ (V,n_{O^+})$[d]	5.66	3.89	⋯	⋯	⋯	⋯	⋯	⋯
$1\,^3B_g\ (V,n_{O^+})$	4.05	4.03	4.97	4.3	5.75	⋯	⋯	⋯
$1\,^1A_u\ (V,n_{O^+})$	3.04	3.06	3.53	3.36	3.92	3.85	⋯	⋯
$1\,^3A_g\ (V,\pi_{C=O^+})$	6.32	5.57	⋯	⋯	⋯	⋯	⋯	⋯
$1\,^3B_u\ (V,n_{O^-})$	4.09	3.65	4.13	3.56	5.31	4.51	4.58	3.63
$1\,^3A_u\ (V,n_{O^+})$	2.62	2.68	2.90	2.73	3.38	3.33	2.86	2.70
$1\,^3B_u\ (V,\pi_{C=O^-})$	5.23	4.01	5.43	3.77	4.09	1.84	5.11	3.12

[a]Reference 19.
[b]References 20, 26, and 61.
[c]Reference 17.
[d]SAC-CI general-*R* calculation.

IX. THE $2\,^1A_g$ STATE

In this work, doubly excited states, so-called $2\,^1A_g$ states, of these three molecules were investigated by the general-*R* method. For butadiene, vertical excitation of this state has been intensively studied by some theoretical works.[30,31] The present calculation predicted the vertical transition energy of 6.56 eV, in agreement with other recent theoretical calculations such as MR-CCCI-PS,[55] DC-MRSDCI,[31] and MR-AQCC.[30] It was important to include up to quadruple excitation operators in the general-*R* calculation. For acrolein, the corresponding state was calculated in the higher energy region at 8.16 eV. The $2\,^1A_g$ states of butadiene and acrolein were characterized as the $\pi\rightarrow\pi^*$ transition with moderate contributions by doubles whose SAC-CI coefficients are ~0.3. On the other hand, the $2\,^1A_g$ state of glyoxal is characterized as pure $(n_{O^+}, n_{O^+}\rightarrow\pi^*, \pi^*)$ double excitation. This is because there is no singly excited state interacting with this state in the same energy region. This $2\,^1A_g$ state of glyoxal was predicted to be very low at 5.66 eV, which is reasonable if we consider the $1\,^3A_u$ state, $n_{O^+}\rightarrow\pi^*$, exist at 2.63 eV. It should be noted that this is the first reliable theoretical calculation of this state to our best knowledge.

The equilibrium structures of these $2\,^1A_g$ states for butadiene and glyoxal were also evaluated by the SAC-CI geometry optimization and the characteristic geometrical changes were predicted. For butadiene, the CC bond length of the $2\,^1A_g$ state increases by 0.102 Å, which is much larger than other singlet states. The same is true for the CO bond length of glyoxal: the CO bond elongation was calculated to be 0.117 Å, while the CC bond length of this state shrinks by 0.156 Å. This large geometrical change is reasonable; the same change was obtained for the $1A_u$ state, $n_{O^+}\rightarrow\pi^*$ transition. The relaxation energies of these states were calculated to be very large, 1.18 and 1.77 eV for butadiene and glyoxal, respectively, which are much larger than other singly excited states.

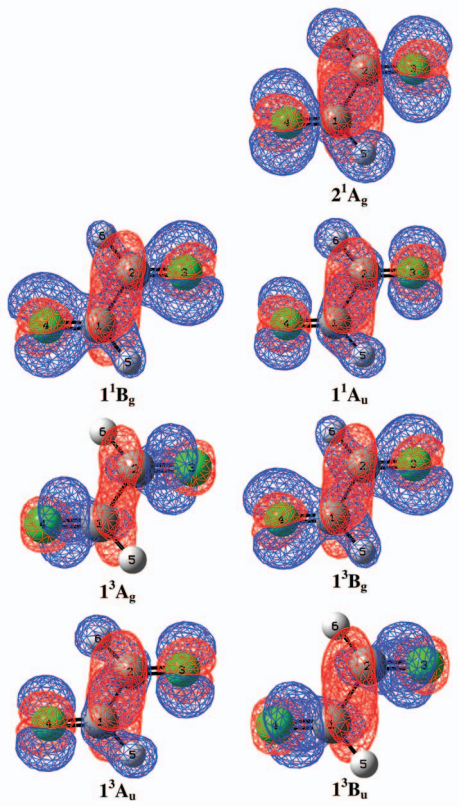

FIG. 6. (Color) SAC-CI electron density difference between the ground and excited states of s-*trans* glyoxal. Blue: decrement; red: increment (interval =0.003).

X. COMPARISON OF THE EXCITED STATES

The calculated excitation energies of vertical singlet and triplet transitions of butadiene, acrolein, and glyoxal are compared in Fig. 7. The valence ionized states are in the order of $\pi_1<\pi_2$ for butadiene, $n<\pi_1<\pi_2$ for acrolein, and $n^+<n^-<\pi_1<\pi_2$ for glyoxal in the increasing order of IPs. Therefore, for butadiene, the low-lying valence excited states are of $\pi\rightarrow\pi^*$ character, while for acrolein and glyoxal, the low-lying states are of $n\rightarrow\pi^*$ character. The transition energy of the lowest $\pi\rightarrow\pi^*$ excitation increases in the order of butadiene, acrolein, and glyoxal, reflecting the IPs of the lowest π states. The correspondence of the $\pi\rightarrow\pi^*$ excitations among these molecules was shown by dotted lines in Fig. 7. In the case of acrolein and glyoxal, the $\pi\rightarrow\pi^*$ tran-

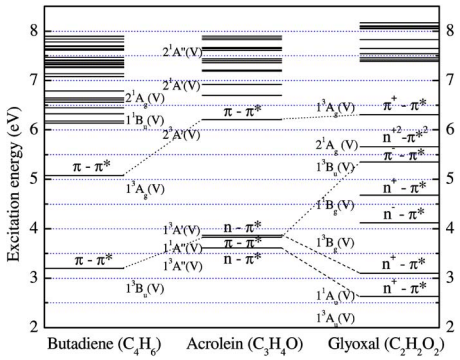

FIG. 7. Comparison among the lowest $\pi \rightarrow \pi^*$ and $n \rightarrow \pi^*$ transitions.

sitions correspond to the excitations from more deeply bound $\pi_{C=O}$ MOs. The lowest $n \rightarrow \pi^*$ transitions of glyoxal are lower in energy than that of acrolein.

XI. CONCLUSION

The SAC-CI method has been successfully applied to calculate the electronic spectra and the excited-state geometries of 1,3-butadiene, acrolein, and glyoxal in their s-*trans* conformation. Theoretical spectra including valence and Rydberg excited states agree well with the experimental spectra and the detailed assignments were proposed with the analysis of second moment. The deviations of the vertical excitation energies from the experiment were less than 0.3 eV for all cases. For the doubly excited states the general-*R* calculations including up to quadruple excitations were performed. The calculated excitation energy of this $2\,^1A_g$ state for butadiene is in good agreement with those of the recent calculations. The $2\,^1A_g$ state of glyoxal was found to be pure double excitation: this is the first reliable theoretical prediction of this state.

The stable structures have been studied for some valence and Rydberg excited states in the planar structure. The optimized ground- and excited-state geometries agree well with the available experimental values; deviations lie within 0.03 Å and 0.7° for the bond lengths and angles, respectively. The geometry relaxation in valence excited states are as large as ~0.1 Å in C–C and C=O bond lengths and those of Rydberg excited states are about ~0.05 Å. For doubly excited states, characteristic geometrical changes and large energetic relaxations were predicted. The force acting on the nuclei caused by the excitations has been discussed in detail by calculating the SAC-CI electron density difference between the ground and excited states; the geometry relaxation was well interpreted in the light of the electrostatic force theory.

ACKNOWLEDGMENTS

This study has been supported by the Grant for Creative Scientific Research from the Ministry of Education, Science and Sports of Japan. One of the authors (B.S.) is grateful to Japan Society for the Promotion of Science (JSPS) for the financial support. The authors thank Professor J. Paldus for the information on the experimental data that were studied in his papers.

[1] A. D. Walsh, Trans. Faraday Soc. **41**, 498 (1945).
[2] W. C. Price and A. D. Walsh, Proc. R. Soc. London, Ser. A **174**, 220 (1940).
[3] A. D. Walsh, Trans. Faraday Soc. **19**, 1425 (1945).
[4] W. M. Flicker, O. A. Mosher, and A. Kuppermann, J. Chem. Phys. **59**, 6502 (1973).
[5] W. M. Flicker, O. A. Mosher, and A. Kuppermann, Chem. Phys. **30**, 307 (1978).
[6] J. P. Doering, J. Chem. Phys. **70**, 3902 (1979).
[7] G. J. Verhaart and H. H. Brongersma, Chem. Phys. Lett. **72**, 176 (1980).
[8] R. McDiarmid, Chem. Phys. Lett. **34**, 130 (1975); A. Fahr and A. K. Nayak, Chem. Phys. **189**, 725 (1994).
[9] J. P. Doering and R. McDiarmid, J. Chem. Phys. **73**, 3617 (1980).
[10] R. McDiarmid, Chem. Phys. Lett. **188**, 423 (1992).
[11] R. R. Chadwick, D. P. Gerrity, and B. S. Hudson, Chem. Phys. Lett. **115**, 24 (1985).
[12] R. S. Becker, K. Inuzuka, and J. King, J. Chem. Phys. **52**, 5164 (1970).
[13] M. Reguero, M. Olivucci, F. Bernardi, and M. A. Robb, J. Am. Chem. Soc. **116**, 2103 (1994); K. W. Paulisse, T. O. Friday, M. L. Graske, and W. P. Polik, J. Chem. Phys. **113**, 184 (2000); M. Olivucci, F. Bernardi, I. N. Ragazos, and M. A. Robb, J. Am. Chem. Soc. **115**, 3710 (1993).
[14] A. C. P. Alves, J. Christoffersen, and J. M. Hollas, Mol. Phys. **20**, 625 (1971).
[15] C. Fridh, L. Asbrink, and E. Lindholm, Phys. Scr. **20**, 603 (1979).
[16] O. Kitao and H. Nakatsuji, Chem. Phys. Lett. **143**, 528 (1988).
[17] S. Shih, R. J. Buenker, and S. D. Peyerimhoff, Chem. Phys. Lett. **16**, 244 (1972).
[18] J. M. Leclerq, C. Mijoule, and P. Yvan, J. Chem. Phys. **64**, 1464 (1976).
[19] K. Hirao, J. Chem. Phys. **79**, 5000 (1983).
[20] C. E. Dykstra, R. R. Lucchese, and H. F. Schaefer III, J. Chem. Phys. **67**, 2422 (1977).
[21] L. Serrano-Andres, M. Merchan, I. Nebot-Gill, R. Lindh, and B. O. Roos, J. Chem. Phys. **98**, 3151 (1993).
[22] L. Serrano-Andres, B. O. Ross, and M. Merchan, Theor. Chim. Acta **87**, 387 (1994).
[23] K. Nakayama, H. Nakano, and K. Hirao, Int. J. Quantum Chem. **66**, 157 (1998).
[24] P. G. Szalay, A. Karpfen, and H. Lischka, Chem. Phys. **130**, 219 (1989).
[25] R. J. Cave and E. R. Davidson, J. Chem. Phys. **91**, 4481 (1987).
[26] C. E. Dykstra and H. F. Schaefer III, J. Am. Chem. Soc. **97**, 7210 (1975).
[27] F. Aquilante, V. Barone, and B. O. Roos, J. Chem. Phys. **119**, 12323 (2003).
[28] H. A. Witek, H. Nakano, and K. Hirao, J. Comput. Chem. **24**, 1390 (2003).
[29] M. Boggio-Pasqua, M. J. Bearpark, M. Klene, and M. A. Robb, J. Chem. Phys. **120**, 7849 (2004).
[30] M. Dallos and H. Lischka, Theor. Chem. Acc. **112**, 16 (2004).
[31] J. Lappe and R. J. Cave, J. Phys. Chem. A **104**, 2294 (2000).
[32] T. Nakajima and H. Nakatsuji, Chem. Phys. Lett. **280**, 79 (1997); Chem. Phys. **242**, 177 (1999).
[33] M. Ishida, K. Toyota, M. Ehara, and H. Nakatsuji, Chem. Phys. Lett. **347**, 493 (2001).
[34] R. Shepard, H. Lischka, P. G. Szalay, T. Kovar, and M. Ernzerhof, J. Chem. Phys. **96**, 2085 (1992); H. Lischka, M. Dallos, and R. Shepard, Mol. Phys. **100**, 1647 (2002).
[35] Y. Luo, H. Ågren, and S. Stafström, J. Chem. Phys. **98**, 7782 (1994).
[36] E. Hollauer and M. A. C. Nascimento, Chem. Phys. Lett. **181**, 463 (1991).
[37] D. W. Turner, *Molecular Photoelectron Spectroscopy* (Wiley-Interscience, New York, NY, 1970).
[38] U. Pincelli, B. Cadloli, and D. J. David, J. Mol. Struct. **9**, 173 (1971); T. Ha, *ibid.* **12**, 171 (1972).
[39] H. Nakatsuji, Chem. Phys. Lett. **59**, 362 (1978).
[40] H. Nakatsuji, Chem. Phys. Lett. **67**, 329 (1979).
[41] H. Nakatsuji, Acta Chim. Hung. **129**, 719 (1992); *Computational Chemistry—Review of Current Trends* (World Scientific, Singapore, 1997); M. Ehara, J. Hasegawa, and H. Nakatsuji, *Theory and Applications of Computational Chemistry: The First 40 Years*, edited by C. E. Dykstra, G. Fenking, K. S. Kim, and G. E. Scuseria (Elsevier, Holland, 2005).
[42] M. Ehara, M. Ishida, K. Toyota, and H. Nakatsuji, *Reviews in Modern Quantum Chemistry*, edited By K. D. Sen (World Scientific, Singapore, 2002); M. Ishida, K. Toyota, M. Ehara, M. J. Frisch, and H. Nakatsuji, J. Chem. Phys. **120**, 2593 (2004).

[43] H. Nakatsuji, J. Am. Chem. Soc. **95**, 345 (1973); H. Nakatsuji and T. Koga, *The Force Concept in Chemistry*, edited by B. M. Deb (Van Nostrand Reinhold, New York, 1981).
[44] T. H. Dunning, J. Chem. Phys. **53**, 2823 (1970).
[45] T. H. Dunning and P. J. Hay, *Methods of Electronic Structure Theory* (Plenum, New York, 1977).
[46] H. Nakatsuji, Chem. Phys. **75**, 425 (1983).
[47] *Structure Data of Free Polyatomic Molecules*, Landolt-Bornstein, New Series, Group II, Vol. 7 (Springer, Berlin, 1976).
[48] H. Nakatsuji, Chem. Phys. Lett. **177**, 331 (1991).
[49] M. J. Frisch, G. W. Trucks, H. B. Schlegel *et al.*, GAUSSIAN 03, Gaussian, Inc., Pittsburgh, PA, 2003.
[50] K. Kimura, S. Katsumata, Y. Achiba, and S. Iwata, *Handbook of Helium(He I) Photoelectron Spectra of Fundamental Organic Molecules. Ionization Energies, ab initio Assignments, and Valence Electronic Structure for 200 Molecules* (Japan Scientific Societies, Tokyo, Japan, 1981).
[51] B. Ostojic and W. Domcke, Chem. Phys. **269**, 1 (2001).
[52] C.-P. Hsu, S. Hirata, and M. Head-Gordon, J. Phys. Chem. A **105**, 451 (2001).
[53] J. P. Doering and R. McDiarmid, J. Chem. Phys. **75**, 2477 (1981).
[54] R. R. Chadwick, D. P. Gerrity, and B. S. Hudson, J. Chem. Phys. **95**, 7204 (1991).
[55] L. Serrano-Andres, J. Sanchez-Mann, and I. Nebot-Gil, J. Chem. Phys. **97**, 7499 (1992).
[56] C. R. Brundle and M. B. Robin, J. Am. Chem. Soc. **92**, 5550 (1970).
[57] R. J. Buenker, S. Shih, and S. D. Peyerimhoff, Chem. Phys. Lett. **44**, 385 (1976).
[58] A. G. Robinson, P. R. Winter, and T. S. Zwier, J. Chem. Phys. **116**, 7918 (2002).
[59] C. S. Page and M. Olivucci, J. Comput. Chem. **24**, 298 (2003).
[60] B. S. Hudson, B. E. Kohler, and K. Schulten, In *Excited States* (Academic, New York, 1982).
[61] C. E. Dykstra and H. F. Schaefer III, J. Am. Chem. Soc. **98**, 401 (1976).
[62] C. E. Bolm and A. Bauder, Chem. Phys. Lett. **88**, 55 (1982).
[63] O. Kitao and H. Nakatsuji, J. Chem. Phys. **87**, 1169 (1987); J. Wan, J. Meller, M. Hada, M. Ehara, and H. Nakatsuji, *ibid.* **113**, 7853 (2000); J. Wan, M. Hada, M. Ehara, and H. Nakatsuji, *ibid.* **114**, 842 (2001).
[64] J. M. Hollas, Spectrochim. Acta **19**, 1425 (1963).
[65] M. Ehara, M. Nakata, and H. Nakatsuji, Mol. Phys. **104**, 971 (2006).
[66] H. L. McMurry, J. Chem. Phys. **9**, 231 (1941).
[67] G. Mackinney and O. Temmer, J. Am. Chem. Soc. **70**, 3586 (1948).
[68] W. Hug, J. Kuhn, K. J. Seibold, H. Labhart, and G. Wag-niere, Helv. Chim. Acta **54**, 1451 (1971).
[69] M. B. Robin, *Higher Excited States of Polyatomic Molecules* (Academic, New York, 1975).
[70] A. D. Walsh, Trans. Faraday Soc. **42**, 66 (1946).
[71] H. Kato, H. Konishi, H. Yamabe, and T. Yonezawa, Bull. Chem. Soc. Jpn. **40**, 2761 (1967).
[72] G. Herzberg, *Molecular Spectra and Structure III. Electronic Spectra and Electronic Structure of Polyatomic Molecules* (Van Nostrand, New York, 1966).
[73] J. C. D. Brand, Trans. Faraday Soc. **50**, 431 (1954).
[74] J. Paldus and D. A. Ramasay, Can. J. Phys. **45**, 1389 (1967).
[75] F. W. Briss, B. D. Braund, A. R. H. Cole, R. Engleman, A. A. Green, S. M. Jarpar, R. Nanes, B. J. Orr, D. A. Ramsay, and J. Szyszka, Can. J. Phys. **55**, 390 (1977).
[76] J. F. Stanton and J. Gauss, Spectrochim. Acta **53**, 1153 (1997).
[77] B. F. Minaev, D. Jonsson, and H. Å. P. Norman, Chem. Phys. **194**, 19 (1995).
[78] E. Drent and J. Kommandeur, Chem. Phys. Lett. **14**, 321 (1972).